75th International Astronautical Congress (IAC), Milan, Italy, 14-18 October 2024.

IAC-24-A3.3A.9

Mars Atmosphere Sounding Balloon: Science Case and System Design

Lars Witte[a]*, Jan Bertram[a], Matthias Grott[b], Caroline Krämer[a], Norbert Toth[a], Torben Wippermann[a]

[a] *German Aerospace Center (DLR), Institute of Space Systems, Bremen / Germany, lars.witte@dlr.de, jan.bertram@dlr.de, caroline.kraemer@dlr.de, norbert.toth@dlr.de, torben.wippermann@dlr.de*
[b] *German Aerospace Center (DLR), Institute of Planetary Research, Berlin / Germany, matthias.grott@dlr.de*
* Corresponding Author

Abstract

Measurements of the state and the variability of the Martian atmosphere significantly contribute to the scientific goal to understand the atmospheric processes on Mars and the engineering goal to prepare for and to de-risk entry, descent and landing operations for future large landing crafts. Balloon-borne instruments could bridge the gap in both temporal and spatial resolution in mesoscale distances between local, stationary landers and global orbiter observations in a similar way as balloon-radiosondes still used today on Earth. The idea to use balloon systems on Mars is not new in essence and has already been proposed in past decades. While those concepts considered an aerial deployment during entry and descent, the concept outlined here revisits a launch off the payload deck of a lander from the Martian surface. This deployment option profits today mainly from the technological advances in micro-electronics and sensor miniaturization which enable designing a balloon-probe significantly smaller than earlier proposed systems. The primary components of the proposed balloon instrument have been subject to testing to mature the concept's critical functions. Particularly, the hull inflation was tested with a subscale model in a low speed wind tunnel to determine the hull's aerodynamic properties in ground proximity and inflation characteristics under wind load. The basic avionic and sensor package has been flown as a radiosonde payload. This paper presents the development status for this instrument and gives further details on the scientific and operational concept, its technical components. It is complemented by the assessment of the risks involved in automatically launching such balloon-system off the Martian surface.

Keywords: Mars exploration; aerobot; scientific ballooning; planetary boundary layer; atmospheric physics

1. Introduction

The planetary boundary layer is the connecting layer between a planet's surface and its atmosphere. Understanding atmospheric processes within this layer is of interest from both a scientific and operational point of view. Convection is believed [1] to be a major transportation process uplifting dust from the surface into the upper atmosphere. In this model, dust is lifted by wind shear at the interface to the soil but remains trapped within the first meters above the surface. Radiative heating and the resulting convective uplift provide a transportation path into higher altitudes where the dust enters planetary scale circulations. Plumes and vortices extend to heights of 5 km to 10 km into the atmosphere. In [2], simulation studies showed that topographic peaks enforce thermal convection with anabatic flows during the daytime, causing plumes to rise beyond the surrounding boundary layer. On the other hand, turbulences caused by such convective instabilities and from the vertical shear of horizontal wind are a potential hazard for approaching landing systems, which have to go through several configuration changes in the breaking process while passing through this final atmospheric layer before touchdown. Previous landings stayed clear of larger topographic formations to circumnavigate potential adverse effects on landing safety from the surface properties itself but also from associated atmospheric hazards [3]. Over the past decades, several numerical atmosphere models with resolutions from global to regional and local came into use. They have been applied to investigate fundamental research questions, including the aforementioned, and to provide mission analysis support for landing and surface missions. Examples are the Mars Weather Research and Forecasting model (MarsWRF, [4]) and the Mars Regional Atmospheric Modeling System (MRAMS, [5]) which have been used for Mars Science Laboratory (MSL) rover landing [6], and Perseverance rover surface and science operation planning [7], as one of the most recent applications. Science and exploration objectives for future missions, however, demand landings closer to such interesting topographic formations [8], which in turn requires a deeper understanding of local and mesoscale weather phenomena at those sites.

The aforementioned analyses are based on numerical simulations and what little in situ observational data is available to validate the underlying models and its predictions. Related investigations obtaining such in situ observational data have been re-quested by the Mars

Exploration Program Advisory Group (MEPAG) in its 2018 update [9]. These are formulated under goal II, "Understand processes of climate of Mars", and goal IV, "Prepare for human exploration".

The concept investigated in this study responds to those stipulated investigations with a balloon-type probe, associated specific research objectives and a suite of sensors as strawman instrumentation. These are outlined in the following chapter. It is worth noting that Martian balloon-system concepts are not new and have been proposed repeatedly over the past decades. Their mission objectives and purposes, however, have changed over time. Early concepts in the pre-rover era, such as the Mars '94/'96 mission proposal [10], considered balloons as platforms to access different sites, including intermittent surface contact, along their flight path for not just meteorologically oriented instrumentation but also instrumentation that nowadays is more meaningfully accommodated with rover missions. The main motivations for revisiting a balloon-probe concept are the ongoing and strong scientific need, specifically from atmospheric sciences, and the enormous progress in the miniaturization of electronics and sensors, which already enabled other aerial platforms such as JPL's Ingenuity helicopter drone [11]. Roles and 'work share' between such drones and balloons or potential 'lighter-than-air' systems are therefore important to clarify, based on their respective capabilities, for upcoming missions and are therefore addressed in the discussion section of this publication. This publication also complements and updates an early description [12] of this balloon-probe.

2. Scientific Concept of Operations and Instrumentation

The investigated experiment concept responds to MEPAG high level investigations with its following instrument objectives:

1. Observe the interaction of the atmosphere with the surface with simultaneous measurements of radiative heat and turbulent fluxes and hence the forcings and effects of the transportation process of dust and other aerosols from the ground into the atmosphere.
2. Monitor the magnitude, spectrum and spatial extent of turbulent zones caused by convective instabilities and vertical shear of the horizontal wind.
3. Provide temporally and spatially highly resolved data usable for validation and improvement of yet numerical model-based predictions of mesoscale phenomena and for validation of orbiter global observational data by measurements of synoptic-scale circulation.

The associated scientific concept of operations is illustrated in Figure 1. Measurements of upwelling radiation ①, using DLR's radiometer technology [13] (Figure 2) flown on the InSight mission, are performed in the 7 to 16 µm wavelength range to determine soil surface temperature, the temperature of the air column underneath the gondola, and the aerosol (dust) content.

Onboard humidity and temperature sensors [14] measure the relative humidity at the balloon altitude. The entire balloon system acts as an 'isopycnic tracer', following the level of constant atmospheric density. Vertical winds force the balloon out of this equilibrium float altitude ②. These vertical wind components and turbulence spectra are measured by baro-integrated inertial data and differential air data around the gondola with a constant temperature anemometer [15]. Large scale horizontal wind components are deduced from the balloon trajectory obtained from radio tracking ③. Balloon position allows correlation of measurements to orographic features and thermo-physical surface properties ④. Altogether, these measurements allow a simultaneous monitoring of key driving forces – thermal gradients, orography – and the magnitude of resulting vertical turbulent fluxes.

The probe shall have a lifetime of at least two Martian days to ensure that repeated diurnal effects can be observed, a diversity of topographic features is crossed and large-scale wind patterns can be resolved. Furthermore, the trajectory shall probe the daytime convective layer which requires a cruising altitude of less than 5000 m above ground level.

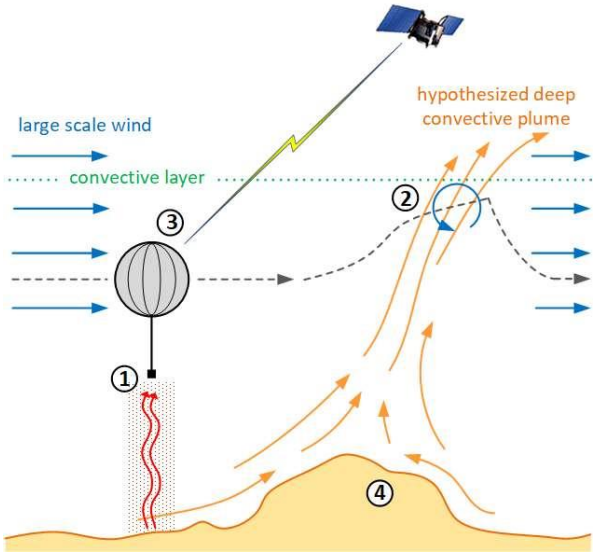

Fig. 1 Illustration of the scientific concept of operations for a probe drifting within the planetary boundary layer. Mission animation on Youtube: youtu.be/stMOdLwX5pw

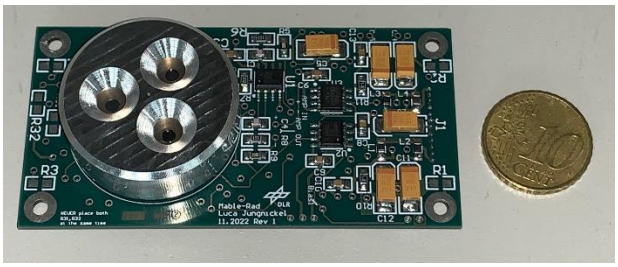

Fig. 2 Three-channel radiometer engineering model

3. Baseline Design and Mission Analysis

The sensor suite is controlled by a system-on-chip onboard computer. Data transmission uses a UHF radio and the CCSDS Proximity 1 Link protocol to enable data relay and tracking by the fleet of Martian orbiters. The avionic is powered by a primary battery, sized to support >50 h of operations. Altogether, the integrated gondola has an estimated mass of ~600 g. A 7 m diameter super-pressure sphere, estimated mass including lifting gas is ~1700 g, is selected to provide a floating altitude of about 2000 m above the MOLA datum. The intended automatized inflation and lift-off sequence requires a hull packing technique which avoids unintended contact with the Martian surface or surrounding spacecraft structure. Hence, any folding pattern which would require unpacking before inflation is unsuitable. In this application, a technique is employed which unfolds the hull during its inflation according to the amount of lifting gas being filled in. Figure 3 shows the instrument configuration (a) with its main components, including the instrument support system, (b) accommodation on a notional lander deck with balloon inflated to a 'ready for launch' state, and (c) the fully inflated balloon probe at ceiling altitude.

The balloon's trajectory depends fundamentally on the date and place of a mission implementation. A balloon flight and systems concept simulator has been implemented to enable a detailed mission analysis for different mission scenarios and/or system configurations.

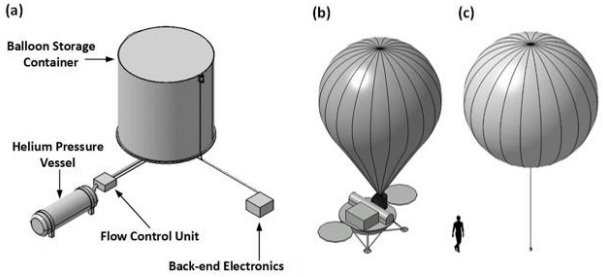

Fig. 3 (a) Principal instrument layout and (b) balloon in launch and (c) flight configuration

3.1 Mission Analysis

The flight dynamics model considers a super-pressure sphere and calculates its motion states, hull pressure and hull volume evolution based on the ambient atmospheric conditions and the lifting gas' thermal state. The flight dynamics model uses equations of motion described in [16]. The thermal state of the system is based on a balloon hull and lifting gas model described in [17] and considers the atmosphere temperature, the direct and reflected solar fluxes, and the surface and sky's thermal radiation at local time of flight. Those environmental parameters are provided by the Mars Climate Database (MCD), version 5.3. The system model in its present form and together with MCD is a flight performance simulator usable for mission and system design. It allows assessments on flight altitude, ranges and directions which can generally be expected based on the global circulation pattern for a given date and site and thereby creating a starting point for this general feasibility assessment.

This analysis assumes, in a 'what-if' scenario, a launch from the ExoMars Rosalind Franklin landing site at Oxia planum at 18.275° N and 24.632° W in the northern summer and winter season with Ls = 60° and Ls = 240° at 04:00 LTST. The simulated flight time is 50 h. Figure 4 shows the prototypical flight profiles of the conceptualized flight system. It ascends to a flight altitude approximately 2000 m above the reference geoid and a height above ground of initially 4000 m. The balloon is taken there by the large-scale winds into a generally southern direction. The trajectories appear as a series of arcs and circles, driven by the diurnal and local circulation pattern and show what generally can be expected in this scenario due to prevailing global circulation and climate. The overflown track distance is nearly 1000 km (summer) and 1900 km (winter). The altitude/elevation chart also displays the predicted ceiling of the daytime convective layer. The flight system's design altitude is deliberately chosen to allow the observation of the convective layer's build-up and passage through its late-day upper extend.

4. Development Tests

The primary components have been subject to testing to demonstrate and mature the concept's critical functions. Particularly, the hull inflation was tested with different subscale models to characterize its properties and behavior during the critical ground proximity phase. These are:

Inflation Testing 1: A (near) half-scale hull with 3.25 m diameter was used to assess manufacturing and integration techniques and to establish folding and packing procedures. Inflation out of its storage container demonstrated its feasibility in a representative scale and proofed compatibility between the hull packing scheme

and the inflation control law. Figure 5 shows this model after an inflation test.

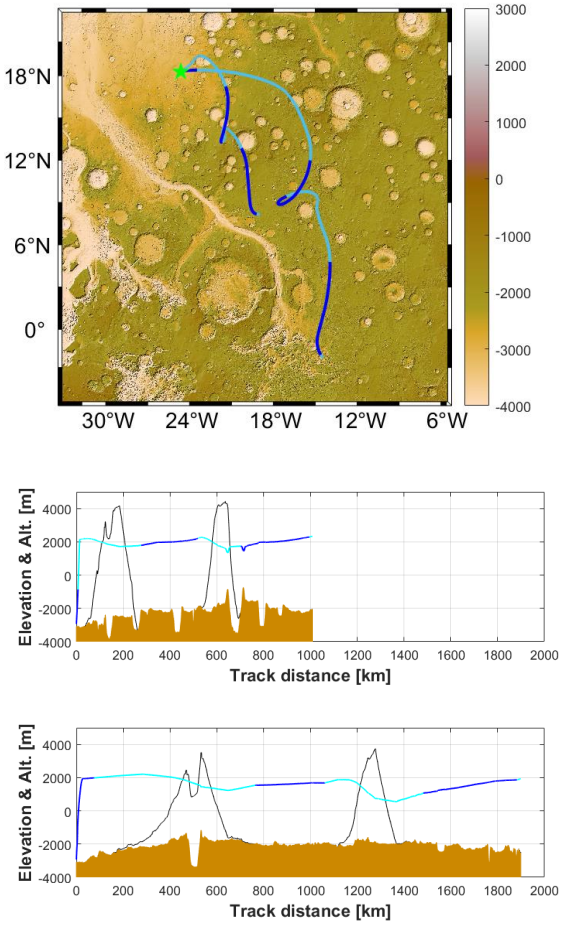

Fig 4 Trajectory simulations for flights during northern summer season (~1000 km, Ls = 60°) and northern winter season (~1900 km, Ls = 240°) for a flight time of 50 h. Balloon launch site in Oxia planum is marked with a green star. Daytime flight segments are colored in light blue and nighttime segment in dark blue, respectively. The altitude/elevation chart displays likewise the flight trajectory in day/night segments. The daytime convective layer vertical extend is indicated in black. This chart is created by using the mapping toolbox from [18].

Inflation Testing 2: A 1 m diameter model hull was designed for use as a wind tunnel test article. Similarity rules satisfy full-scale (7 m) hull forces balance on Mars. The wind tunnel tests, conducted at the DNW Low Speed Wind Tunnel facility in Braunschweig, Germany (Figure 6), served two objectives:

1. Proofing the inflation technique and Characterization of the hull inflation dynamics under expected Mars wind load
2. Determine the hull's aerodynamic properties of its static and dynamic blow-down and vortex induced vibrations in ground proximity.

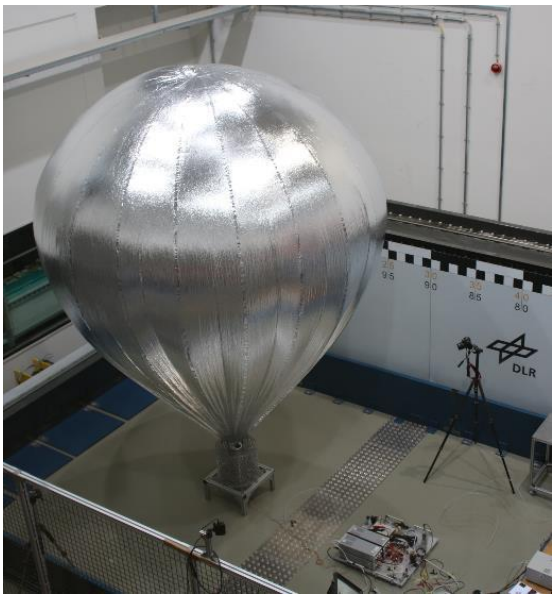

Fig. 5 A 3.25 m test sphere in DLR's Landing and Mobility Test Facility LAMA.

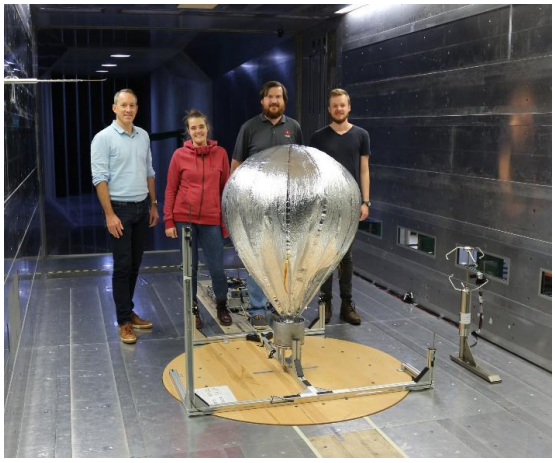

Fig. 6 A 1.0 m test sphere in the DNW Low Speed Wind Tunnel.

The image sequence shown in Figure 7 shows an auto-inflation test with a wind tunnel wind speed of 2.5 m/s, referring to 4.0 m/s on Mars (a dedicated, peer-reviewed journal article covering this test set-up and results is currently under preparation).

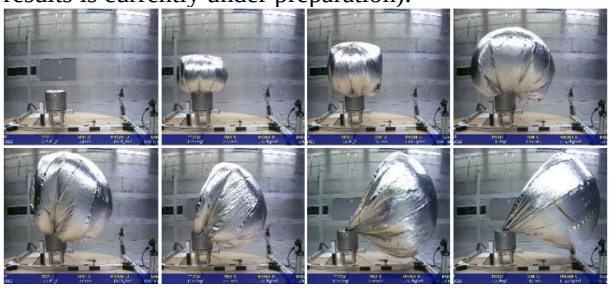

Fig 7 Inflation image sequence obtained during wind tunnel tests

Avionic Flight Tests: The avionic breadboard has been subject to flight tests with yet more engineering driven objectives to

- investigate avionics function in (near) representative pressure, temperature and time scale, and to
- acquire sensor data sets in a real meteorological (but not Mars analogue) context

The experimental campaigns, set-ups seen in Figure 8 were split into two types of test to cover the flight regime of interest. These are (a) a 48h-long duration, but stationary tethered flight and (b) a short duration 3 h free-flight as radiosonde with an altitude of approximately 20 km.

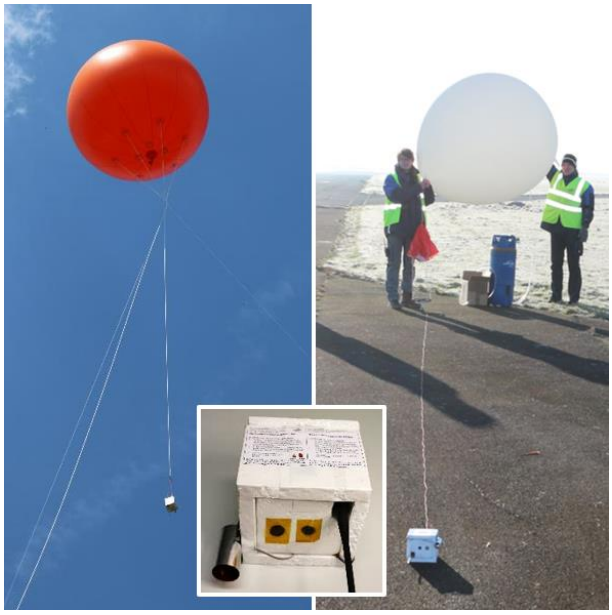

Fig. 8 First core avionic and basic instrumentation tests in a stationary, tethered (left) and free-flight conditions as radiosonde (right)

5. Deployment Safety & Risk Mitigation

The balloon hull extraction and inflation process is probably the most critical singular event to be mastered in any balloon mission sequence. The sequence (Figure 7) shows that at a certain point the entire hull gets out of the container while lifting gas is still being supplied until reaching its target lifting gas load. This release occurs when exceeding an inflation ratio of $I_R = 50$ %. After this period, the hull is susceptible to being blown against surrounding objects on the ground or adjacent parts of the lander spacecraft by the surface winds. Contrarily, the maximum allowable blow-down angle is constrained by the available obstacle free safety cone (Figure 9) of the hosting spacecraft, which is a major limiting factor for the safe wind speed limit.

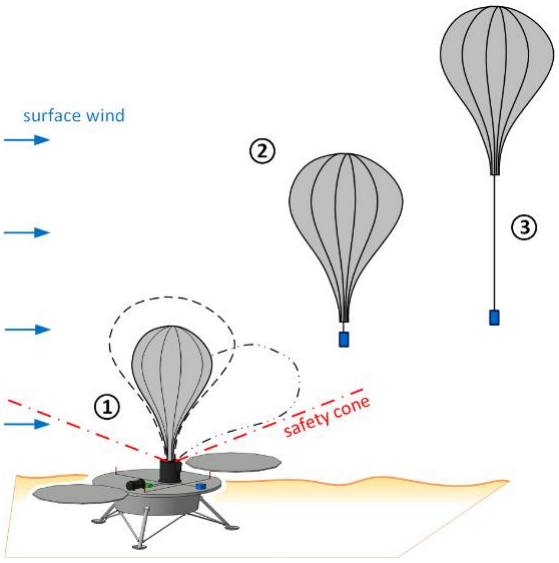

Fig. 9 Illustration of launch concept of operations: (1) wind speed limit is constrained by obstacle-free cone around balloon support system, (2) release with retracted gondola, and (3) unreeling of suspension line when clear of ground.

Based on the wind tunnel test results, the dynamic blow-down angle is determined for the 7 m-hull's mass distribution, its drag, lift and buoyancy, as a function of the momentary inflation ratio.

Figure 10 shows the blow-down angle of the partially inflated (minimum inflation ration $I_R = 50$ %) balloon hull in response to surface wind. The blow-down angle is defined as angle between local gravity vector and the hull's axis connecting the hull's root cone and tip apex. The balloon hull oscillates around its static blow-down angle (dashed line) due to turbulence and vortex-induced vibrations (VIV). The resultant dynamic peak blow-down angle (solid line) shows a peak at about 1.5 m/s when VIV are in the resonance region. The underlying fundamental aerodynamics and equations are investigated in [19] with application to tethered balloons described in [20]. The following analysis is based on these fundamentals with aerodynamic data (unpublished yet) obtained from the wind tunnel tests mentioned in chapter 4 above. The ultimate blow-down angle is reached when the hull's lower limb crosses the horizontal plane. This marks the begin of the 'unsafe' regime and defines the associated wind velocity. A 20 % margin on the ultimate dynamic blow-down angle is defined here as 'safe regime' with an associated wind velocity of ~ 3.2 m/s. Higher inflation ratios lead to higher wind tolerances. The consequential following question is where and when this limit can be reliably met.

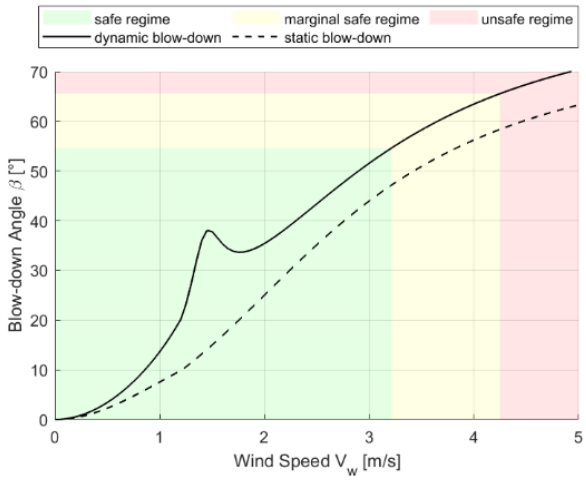

Fig. 10 Dynamic Blow-down angle envelope as a function of wind speed for a 50% inflated balloon hull. Safe regime retains 20 % margin towards the full blow-down of the hull's lower limb.

The probability of achieving a deployment below a safe wind speed limit V_{wlim} can be assessed by using a metric also known as "survivability" [21]. The probability P_{safe} (Equation (1)) of being inside safe wind limits is expressed as "not being unsafe", where P_{unsafe} is determined by the susceptibility to adverse wind conditions, denoted as P_s, and vulnerability to those conditions, denoted as P_v.

$$P_{safe} = 1 - P_{unsafe} = 1 - P_v \cdot P_s \qquad (1)$$

Previous Mars surface missions have provided meteorological data sets for surface winds which allow us to derive weather statistics which can be used to estimate the probability of exceeding a certain wind speed limit V_{wlim}. The frequency of occurrence of certain wind speeds within an observation period can be described by the Weibull distribution function. Accordingly, the probability that a prevailing wind speed exceeds the wind speed limit is expressed by Equation (2) with the Weibull distribution parameters c, being the scale wind speed [m/s], and k, being a dimensionless shape parameter.

$$P_s = P(V_w > V_{wlim}) = e^{-(V_{wlim}/c)^k} \qquad (2)$$

Its application as a Mars surface wind model is discussed in [22], and Viking lander hourly averaged wind data was evaluated to provide estimates of the scale and shape parameter for the Viking sites. Those estimates are over observation episodes of several days. Similar analyses were published in [23] for the Mars Science Laboratory's Gale crater site, taking profit of higher frequent measurements of its environment monitoring station. The higher sampling rate provides a better resolution of the unsteadiness in the prevailing wind. Diurnal variations are accounted for by selecting the observation episodes as windows of several hours, whose duration is denoted here with the parameter w. Within an observation period, the likelihood of occurrence over time is uniform, meaning it disregards the preference of certain winds towards a point in time within that period. The resulting probability to be exposed to a certain wind condition is given by Equation (3) where d denotes the duration of inflation.

$$P_v = d/w \qquad (3)$$

Consequently, the probability to stay inside safe limits can be increased by designing for a higher wind tolerance (larger V_{wlim}) and/or to avoid adverse wind conditions my minimizing the exposure time with a short inflation duration d. The resulting probabilities as functions of the parameters V_{wlim} and d are plotted in Figure 11. As an example, this set of curves is based on the Weibull distribution parameters c = 5.29 m/s and k = 1.95, taken from [23], notionally assuming wind condition as observed in the Gale crater in a 00:00 to 03:00 LTST nighttime period. The analyses given in [22,23] indicate that the northern hemisphere spring season and nighttime provide generally the most favorable wind conditions for balloon launch operations.

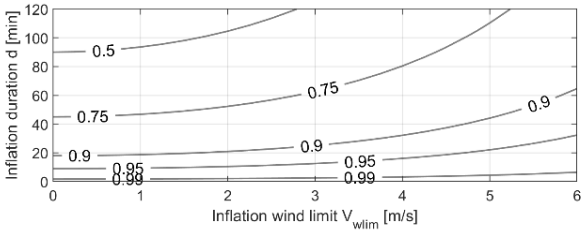

Figure 11 Iso-lines represent achievable probabilities to stay below the associated wind speeds and as function of the deployment duration.

Read-out example: To achieve a probability of better than 95 % to stay within a 3 m/s wind speed limit, an inflation duration from I_R = 50 % to the launch I_R ~ 66 % of 10 minutes or less would be required.

The risk of an unsuccessful deployment is determined by the probability of an unsafe deployment and the severity level of such an event. The worst-case outcome of an unsafe deployment would be not just a failure of the balloon mission itself but the potential catastrophic impairment of the hosting mission by entanglement of the balloon hull with the carrier spacecraft. The corresponding mitigation strategy must be developed in a mission-specific context and could comprise design and operational measures such as detaching and depositing the whole balloon launch system from the main spacecraft for a launch at a safe distance. Alternatively, if staying on the hosting spacecraft, the balloon launch could be scheduled at the final end of the main mission's timeline.

6. Discussion & Conclusions

The scientific rationale for this concept stems from the high priority investigations required by MEPAG. Specific investigations relate to the highly variable Mars Boundary Layer (MBL) and the direct interaction between the surface and the lower atmosphere. While orbital experiments to study the Martian lower atmosphere and meteorological analyses aboard landers are well established, there are no in situ measurements (temperature, pressure, humidity, dust opacity, wind properties, etc.) of the state of the near-surface lower atmosphere between 1 to 10 km altitude except for results during the descent of some lander probes. These investigations can be addressed with a balloon probe drifting through the atmospheric boundary layer, filling the gap in temporal and spatial coverage between global orbiter surveyance and local observations by stationary landers or shorter-ranged rover/drones. The wind drifting is part of the sensing principle as the balloon acts as a 'tracer' to resolve the large-scale wind pattern. The role sharing with powered vehicles or drones is therefore complementary, but not competitive. The choice of such a probe for this purpose is driven by the science case and not for technology demonstration in the first hand. A strawman sensor suite suitable for serving the outlined scientific concept of operations is based on state-of-the-art, proven technology. Nevertheless, the balloon system itself involves the implementation of technologies not yet demonstrated in the context of Mars exploration, whose demonstration could pave the way for more advanced lighter-than-air vehicles or aerobots.

The conceptual design and the mission simulation show that the proposed balloon probe could roam the Martian boundary layer for at least two days. Lander and rover missions have acquired large data sets of surface meteorological conditions over the past decades. Derived surface wind statistics allow for a quite clear view on the conditions to be expected on the Martian surface and enable a design for a balloon launch off the surface.

The proposed deployment risk analysis scheme supports a managed and risk-informed design and operational concept development. It provides the nucleus for trade-offs between deployment wind speed limits, available obstacle free instrument accommodation options, inflation process design parameters, expected landing site surface wind environment and programmatically required safety levels. The aerodynamic coefficients describing the forces acting on the balloon hull during inflation under wind conditions have been characterized in a dedicated wind tunnel test campaign.

The achieved level of definition of this probe concept and lack of specific hosting mission context, however, do not allow a firm statement of mission readiness yet. Hence, this concept should not be regarded as a 'proposal' in a programmatic sense. However, with all due respect to the remaining uncertainties, this feasibility study concludes that such a balloon probe mission is in reach of technical possibility.

References

[1] Newman, C.E.; Lewis, S.R.; Read, P.L.; Forget, F. Modeling the Martian Dust Cycle, 1. Representations of Dust Transport Processes. J. Geophys. Res. 2002, 107, 6-1–6-18. https://doi.org/10.1029/2002JE001910.

[2] Rafkin, S.C.R. The Potential Importance of Non-Local, Deep Transport on the Energetics, Momentum, Chemistry, and Aerosol Distributions in the Atmospheres of Earth, Mars, and Titan. Planet. Space Sci. 2012, 60, 147–154. https://doi.org/10.1016/j.pss.2011.07.015.

[3] Rafkin, S.C.R.; Michaels, T.I. Meteorological Predictions for 2003 Mars Exploration Rover High-Priority Landing Sites: Meteorological Predictions for Mer. J. Geophys. Res. 2003, 108, 8091. https://doi.org/10.1029/2002JE002027.

[4] Toigo, A.D.; Lee, C.; Newman, C.E.; Richardson, M.I. The Impact of Resolution on the Dynamics of the Martian Global Atmosphere: Varying Resolution Studies with the MarsWRF GCM. Icarus 2012, 221, 276–288. https://doi.org/10.1016/j.icarus.2012.07.020.

[5] Rafkin, S.; Michaels, T. The Mars Regional Atmospheric Modeling System (MRAMS): Current Status and Future Directions. Atmosphere 2019, 10, 747. https://doi.org/10.3390/atmos10120747.

[6] Vasavada, A.R.; Chen, A.; Barnes, J.R.; Burkhart, P.D.; Cantor, B.A.; Dwyer-Cianciolo, A.M.; Fergason, R.L.; Hinson, D.P.; Justh, H.L.; Kass, D.M.; et al. Assessment of Environments for Mars Science Laboratory Entry, Descent, and Surface Operations. Space Sci. Rev. 2012, 170, 793–835. https://doi.org/10.1007/s11214-012-9911-3.

[7] Pla-García, J.; Rafkin, S.C.R.; Martinez, G.M.; Vicente-Retortillo, Á.; Newman, C.E.; Savijärvi, H.; de la Torre, M.; Rodriguez-Manfredi, J.A.; Gómez, F.; Molina, A.; et al. Meteorological Predictions for Mars 2020 Perseverance Rover Landing Site at Jezero Crater. Space Sci. Rev. 2020, 216, 148. https://doi.org/10.1007/s11214-020-00763-x.

[8] Kerr, R.A. Safety Versus Science on Next Trips to Mars. Science 2002, 296, 1006–1008. https://doi.org/10.1126/science.296.5570.1006.

[9] Banfield, D. (Ed.) MEPAG, Mars Scientific Goals, Objectives, Investigations, and Priorities: 2018; White Paper Posted October, 2018 by the Mars Exploration Program 2018; MEPAG Goals Committee: Pasadena, CA, USA, 2018. Available online:

https://mepag.jpl.nasa.gov/reports/MEPAG%20Goals_Document_2018.pdf (accessed on 21.02.2020).

[10] Vargas, A.; Evrard, J.; Mauroy, P. Mars 96 Aerostat—An Overview of Technology Developments and Testing. In Proceedings of the International Balloon Technology Conference, San Francisco, CA, USA, 3 June 1997; American Institute of Aeronautics and Astronautics: Reston, VA, USA, 1997.

[11] Balaram, J.; Aung, M.; Golombek, M.P. The Ingenuity Helicopter on the Perseverance Rover. Space Sci. Rev. 2021, 217, 56. https://doi.org/10.1007/s11214-021-00815-w.

[12] Witte, L.; Arnold, G.; Bertram, J.; Grott, M.; Krämer, C.; Lorek, A.; Wippermann, T. A Concept for a Mars Boundary Layer Sounding Balloon: Science Case, Technical Concept and Deployment Risk Analysis. Aerospace 2022, 9, 136. https://doi.org/10.3390/aerospace9030136

[13] Spohn, T.; Grott, M.; Smrekar, S.E.; Knollenberg, J.; Hudson, T.L.; Krause, C.; Müller, N.; Jänchen, J.; Börner, A.; Wippermann, T.; et al. The Heat Flow and Physical Properties Package (HP3) for the InSight Mission. Space Sci. Rev. 2018, 214, 96. https://doi.org/10.1007/s11214-018-0531-4.

[14] Lorek, A.; Majewski, J. Humidity Measurement in Carbon Dioxide with Capacitive Humidity Sensors at Low Temperature and Pressure. Sensors 2018, 18, 2615. https://doi.org/10.3390/s18082615.

[15] Domínguez-Pumar, M.; Kowalski, L.; Jiménez, V.; Rodríguez, I.; Soria, M.; Bermejo, S.; Pons-Nin, J. Analyzing the Performance of a Miniature 3D Wind Sensor for Mars. Sensors 2020, 20, 5912. https://doi.org/10.3390/s20205912.

[16] Abe, T.; Imamura, T.; Izutsu, N.; Yajima, N. Scientific Ballooning; Springer: New York, NY, USA, 2009; ISBN 978-0-387-09725-1978-0-387-09727-5.

[17] Farley, R. BalloonAscent: 3-D Simulation Tool for the Ascent and Float of High-Altitude Balloons. In Proceedings of the AIAA 5th ATIO and 16th Lighter-Than-Air Systems Technology and Balloon Systems Conferences, Arlington, VA, USA, 26 September 2005; American Institute of Aeronautics and Astronautics: Reston, VA, USA, 2005.

[18] Pawlowicz, R. M_Map: A Mapping Package for MATLAB; version 1.4m; Computer software; 2020. Available online: www.eoas.ubc.ca/~rich/map.html (last accessed on 03.03.2022)

[19] Govardhan, R. N.; Williamson, C. H. K., Vortex-induced vibrations of a sphere. J. Fluid Mech. 2005, vol. 531, pp. 11–47. https://doi.org/10.1017/S0022112005003757

[20] Coulombe-Pontbriand, P., Nahon M., Experimental testing and modeling of a tethered spherical aerostat in an outdoor environment, J. Wind Eng. Ind. Aerodyn. 2009, 97, 5–6, p. 208-218, https://doi.org/10.1016/j.jweia.2009.06.005.

[21] Soban, D.; Mavris, D. Methodology for Assessing Survivability Tradeoffs in the Preliminary Design Process. In Proceedings of the 2000 World Aviation Conference, San Diego, CA, USA, 10 October 2000; American Institute of Aeronautics and Astronautics: Reston, VA, USA, 2000.

[22] Lorenz, R.D. Martian Surface Wind Speeds Described by the Weibull Distribution. J. Spacecr. Rocket. 1996, 33, 754–756. https://doi.org/10.2514/3.26833.

[23] Viúdez-Moreiras, D.; Gómez-Elvira, J.; Newman, C.E.; Navarro, S.; Marin, M.; Torres, J.; de la Torre-Juárez, M. Gale Surface Wind Characterization Based on the Mars Science Laboratory REMS Dataset. Part II: Wind Probability Distributions. Icarus 2019, 319, 645–656. https://doi.org/10.1016/j.icarus.2018.10.010.